Bio-Inspired 3D Flocking Algorithm with Minimal Information Transfer for Drones Swarms

Matthieu Verdoucq, Clément Sire, Ramón Escobedo, Guy Theraulaz, Gautier Hattenberger

▶ **To cite this version:**

Matthieu Verdoucq, Clément Sire, Ramón Escobedo, Guy Theraulaz, Gautier Hattenberger. Bio-Inspired 3D Flocking Algorithm with Minimal Information Transfer for Drones Swarms. 2023 IEEE/RSJ International Conference on Intelligent Robots and Systems (IROS), IEEE, pp.8833-8838, 2023, 10.1109/IROS55552.2023.10341413 . hal-04357875

HAL Id: hal-04357875

https://enac.hal.science/hal-04357875v1

Submitted on 21 Dec 2023

HAL is a multi-disciplinary open access archive for the deposit and dissemination of scientific research documents, whether they are published or not. The documents may come from teaching and research institutions in France or abroad, or from public or private research centers.

L'archive ouverte pluridisciplinaire **HAL**, est destinée au dépôt et à la diffusion de documents scientifiques de niveau recherche, publiés ou non, émanant des établissements d'enseignement et de recherche français ou étrangers, des laboratoires publics ou privés.

Bio-inspired 3D flocking algorithm with minimal information transfer for drones swarms

Matthieu Verdoucq[1,2,*], Clément Sire[3], Ramón Escobedo[2], Guy Theraulaz[2], and Gautier Hattenberger[1]

[1]École Nationale de l'Aviation Civile, Université de Toulouse, 31400 Toulouse, France
[2]Centre de Recherches sur la Cognition Animale, Centre de Biologie Intégrative (CBI), CNRS & Université de Toulouse – Paul Sabatier, 31062 Toulouse, France
[3]Laboratoire de Physique Théorique, CNRS & Université de Toulouse – Paul Sabatier, 31062 Toulouse, France

***Abstract*— This article introduces a bio-inspired 3D flocking algorithm for a drone swarm, built upon a previously established 2D model, which has proven to be effective in promoting stability, alignment, and distance variation between agents within large groups of agents. The study highlights how the incorporation of a vertical interaction between agents and the acquisition by each agent of a minimal amount of information about their most influential neighbor impacts the collective behavior of the swarm. Additionally, we present a comprehensive investigation of the impacts of the intensity of alignment and attraction interactions on the collective motion patterns that emerge at the group level. These results, mostly conducted in a validated simulator, have significant implications for designing efficient UAV swarm systems and using collective patterns, or phases, in operational contexts such as corridor tracking, surveillance, and exploration. Further research will explore the effectiveness and efficiency of this UAV swarm flocking algorithm, as well as its ability to ensure safe transitions between collective phases in different operational contexts.**

***Index Terms*— 3D Flocking Algorithm, Collective Motion, Distributed Control, Drone Swarm, Unmanned Aerial Vehicle (UAV)**

I. Introduction

Drones, or unmanned aerial vehicles (UAVs), have become increasingly popular in recent years and are being used in a wide range of applications, including surveillance, mapping, delivery, and search and rescue [1], [2], [3]. One key challenge in operating a swarm of drones is guidance: how to coordinate the movements of multiple drones to achieve a desired task or objective. Swarm systems often implement agent and obstacle avoidance coupled with navigation toward an objective [4] or structural formation within the group [5]. However, bio-inspired algorithms, which are based on models of collective behaviors observed in group-living animals (e.g., social insects, fish schools, and flocks of birds), have emerged as a promising approach to control a swarm of drones due to their ability to rapidly adapt to changing environments and self-organize into complex patterns [6]. In a previous work [7], we developed a 2D flocking algorithm for a swarm of drones based on a model describing the collective behavior of fish [8], [9], [10]. Here, we introduce a 3D version of this flocking algorithm, and we describe its implementation in a swarm of drones, its validation in an indoor flight arena, as well as in simulations. In section III-B, we also discuss the impact of adding a vertical interaction between agents in the model on the resulting swarm behavior, and in particular, the emergence of vertical movement patterns. The potential applications and their benefits in an operational context are also discussed, through the exploitation of different collective phases during a mission. Except for the results presented in Fig. 4, all results presented here are produced in simulation, using the ROS2 [11] framework, formerly validated on a swarm of drones inside an indoor flying arena in [7].

* Corresponding author: matthieu.verdoucq@enac.fr

II. 3D flocking algorithm

Consider a swarm of N UAVs flying in a planar space. The instantaneous state of the UAV i is determined by the vector $\vec{U}_i(t) = (\vec{u}_i(t), \phi_i(t))$, where $\vec{u}_i = (x_i, y_i, z_i)$ and ϕ_i denote the UAV's position and heading angle, respectively. The velocity vector is $\vec{v}_i = (v_i^x, v_i^y, v_i^z)$. Then, the command vector can be written as $\vec{V}_i(t) = (\mathrm{v}_i(t), v_i^z(t), \omega_i(t))$, where $\mathrm{v}_i = \|(v_i^x, v_i^y)\|$ is the longitudinal speed and ω_i the angular turning rate, both calculated with a PID controller according to the environmental and social interactions of the UAV and a given target heading. We have:

$$\dot{\vec{U}}_i(t) = \big(\vec{v}_i(t), \omega_i(t)\big). \tag{1}$$

Agent's speed and heading variation $\delta\vec{V}_i$ is updated at a fixed frequency and according to the social interactions with other agents (soc), the effect of the upper, lower and side borders of the cylindrical arena (border), and the operational goal that includes an attraction to a given altitude (nav):

$$\delta\mathrm{v}_i = \delta\mathrm{v}_i^{\mathrm{soc}} + \delta\mathrm{v}_i^{\mathrm{border}} + \delta\mathrm{v}_i^{\mathrm{nav}}, \tag{2}$$

$$\delta v_i^z = (\delta v_i^z)^{\mathrm{soc}} + (\delta v_i^z)^{\mathrm{border}} + (\delta v_i^z)_{\|} + (\delta v_i^z)^{\mathrm{nav}}, \tag{3}$$

$$\delta\phi_i = \delta\phi_i^{\mathrm{soc}} + \delta\phi_i^{\mathrm{border}} + \delta\phi_i^{\mathrm{nav}}. \tag{4}$$

Social terms are $\delta\mathrm{v}_i^{\mathrm{soc}} = \sum_{j\in J}\delta\mathrm{v}_{ij}$, $(\delta v_i^z)_{\mathrm{soc}} = \sum_{j\in J}\delta v_{ij}^z$, and $\delta\phi_i^{\mathrm{soc}} = \sum_{j\in J}(\phi_{ij}^{\mathrm{Ali}} + \phi_{ij}^{\mathrm{Att}})$, where J is the set of agents with which agent i interacts (typically 1 or 2). They are given by pairwise functions describing the effect of longitudinal

speed, vertical speed, alignment, and attraction, respectively:

$$\delta \mathrm{v}_{ij} = \gamma_{\mathrm{Acc}} \cos(\psi_{ij}) \big(d_0^{\mathrm{v}} - d_{ij}^{\mathrm{c}}\big) \left(1 + \frac{d_{ij}^{\mathrm{c}}}{l_{\mathrm{Acc}}}\right)^{-1}, \quad (5)$$

$$\delta v_{ij}^{z} = \gamma_{\mathrm{z}} \left[\tanh\left(\frac{d_{ij}^{\mathrm{z}}}{a_z}\right) + \tanh\left(\frac{d_{ij}^{\mathrm{z}} - d_0^z}{a_z}\right)\right] \times \exp\left[-\left(\frac{d_{ij}^{\mathrm{c}}}{L_{z_2}}\right)^2\right], \quad (6)$$

$$\delta \phi_{ij}^{\mathrm{Ali}} = \gamma_{\mathrm{Ali}} (d_{ij}^{\mathrm{c}} + d_0^{\mathrm{Ali}}) \exp\left[-\left(\frac{d_{ij}^{\mathrm{c}}}{l_{\mathrm{Ali}}}\right)^2\right] \sin(\phi_{ij}) \times \big(1 + \alpha_{\mathrm{Ali}} \cos(\psi_{ij})\big)[1 - f_{\mathrm{w}}(r_{\mathrm{w}})], \quad (7)$$

$$\delta \phi_{ij}^{\mathrm{Att}} = \gamma_{\mathrm{Att}} (d_{ij}^{\mathrm{c}} - d_0^{\mathrm{Att}}) \left[1 + \left(\frac{d_{ij}^{\mathrm{c}}}{l_{\mathrm{Att}}}\right)^2\right]^{-1} \sin(\psi_{ij}) \times \big(1 + \alpha_{\mathrm{Att}} \cos(\psi_{ij})\big)[1 - f_{\mathrm{w}}(r_{\mathrm{w}})] q(d_{ij}^{\mathrm{c}}). \quad (8)$$

These functions depend on five variables characterizing the geometrical state of pairs of agents ij: the coupling distance d_{ij}^{c} separating them, the angle ψ_{ij} with which i perceives j, their heading difference ϕ_{ij}=$\phi_j - \phi_i$, the vertical distance d_{ij}^{z}, and the distance to the wall in the horizontal plane r_{w}. The parameters of these functions are their respective strength γ_{Acc}, γ_{z}, γ_{Ali}, γ_{Att}, their respective distance of equilibrium d_0^{v}, d_0^z, d_0^{Ali}, d_0^{Att}, and their respective range of action, determined respectively by l_{Acc}, a_z, L_{z_2}, l_{Ali}, and l_{Att}. The function f_{w} reduces the strength of the interaction when the agent is close to the wall, and $q(d) = 2d/(4d - d_0^{\mathrm{Att}})$, if $d \leq d_0^{\mathrm{Att}}$, and $q(d) = 1$, if $d > d_0^{\mathrm{Att}}$. Finally, α_{Ali} and α_{Att} are normalization constants for the angular functions of interaction. The coupling distance between agents d_{ij}^{c} is a weighted distance, where the effective range of the interaction is larger by a factor σ_z along the Z-axis (we used $\sigma_z = \sqrt{2}$) to prevent collisions or failures between vertically aligned agents due to the columns of air perturbations that are produced by multirotors:

$$d_{ij}^{\mathrm{c}} = \sqrt{(x_i - x_j)^2 + (y_i - y_j)^2 + (z_i - z_j)^2/\sigma_z^2}. \quad (9)$$

Recent findings in social fish have shown that each individual acquires a minimal amount of information about a limited number of neighbors (typically one or two) to coordinate movements at the group level, thus facilitating decision-making processes and preventing cognitive overload [12], [13]. This feature is included in our model by selecting the number and identity of agents each drone interacts with, thus reducing the amount of information that has to be processed. The interacting neighbors are precisely those that exert the highest influence on the focal agent, where the influence that agent j exerts on agent i is given by the cost function

$$I_{ij}(t) = \sqrt{(\delta \mathrm{v}_i)^2 + (\delta v_i^z)^2 + (\delta \phi_i \mathrm{v}_i)^2}. \quad (10)$$

The operational terms $\delta \mathrm{v}_i^{\mathrm{nav}}$, $(\delta v_i^z)^{\mathrm{nav}}$ and $\delta \phi_i^{\mathrm{nav}}$ serve to determine the guiding strategy for the swarm to adopt a given position, speed, and heading. Here only $(\delta v_i^z)^{\mathrm{nav}}$ is used, to attract drones towards a specified altitude z_{alt}:

$$(\delta v_i^z)^{\mathrm{nav}} = -\gamma_{\perp} \tanh\left(\frac{z - z_{\mathrm{alt}}}{a_z}\right). \quad (11)$$

$$(\delta v_i^z)^{\mathrm{border}} = \frac{\gamma_{\perp}}{\frac{1 + \exp\left[d_{z_{border}}\right]}{d_{z_0}}} \quad (12)$$

with $d_{z_{border}}$

Finally,

$$(\delta v_i^z)_{\parallel} = -\gamma_{\parallel} \times v_i^z / \left\| v_i \right\|, \quad (13)$$

is used to smooth abrupt changes in the vertical direction.

Expressions (2)-(13) are the generalization to a 3D framework of the interactions introduced in the 2D-model [7].

III. Impact of the vertical interaction on collective behaviors

A. 3D collective behaviors

In fish schools, the collective motion patterns that emerge from social interactions are called phases, in analogy with physical matter states or phases (e.g., gas, liquid, solid...) [14]. The flocking algorithm can generate a variety of identifiable 3D patterns of collective movements, depending on the value of the interaction strengths γ_{Ali} and γ_{Att}. We characterize these patterns by means of three observables quantifying the behavior and the spatial distribution of the agents:

- The group dispersion $D(t)$, measuring the level of cohesion of the group and corresponding to the mean 3D distance of the UAVs to the barycenter of the swarm B:

$$D(t) = \sqrt{\frac{1}{N} \sum_{i=1}^{N} \|\vec{u}_i - \vec{u}_B\|^2}. \quad (14)$$

- The polarization $P(t)$ of the swarm, corresponding to the degree of alignment of the agents:

$$P(t) = \frac{1}{N} \left\| \sum_{i=1}^{N} \vec{e}_i(t) \right\| \in [0, 1], \quad (15)$$

with $\vec{e}_i = \vec{v}_i / \|\vec{v}_i\|$ being the unit vector of agent's heading. High values of P mean that agents are aligned and point in the same direction. Small values of P mean that agents point in different directions, but polarization can be correlated to the number of agents if it is low (uncorrelated movement would result in $P \sim 1/\sqrt{N}$).

- The milling index $M(t)$ of the swarm, measuring how much the agents are turning around their barycenter, and in the same direction:

$$M(t) = \left| \frac{1}{N} \sum_{i=1}^{N} \sin(\bar{\theta}_{\mathrm{w}}^i(t)) \right| \in [0, 1], \quad (16)$$

with $\bar{\theta}_{\mathrm{w}}^i = \bar{\phi}_i - \bar{\theta}_i$. Variables with a bar are defined in the barycenter system of reference. The milling index can also be defined with respect to a specific point other than the barycenter (e.g., characterizing the swarm behavior inside a

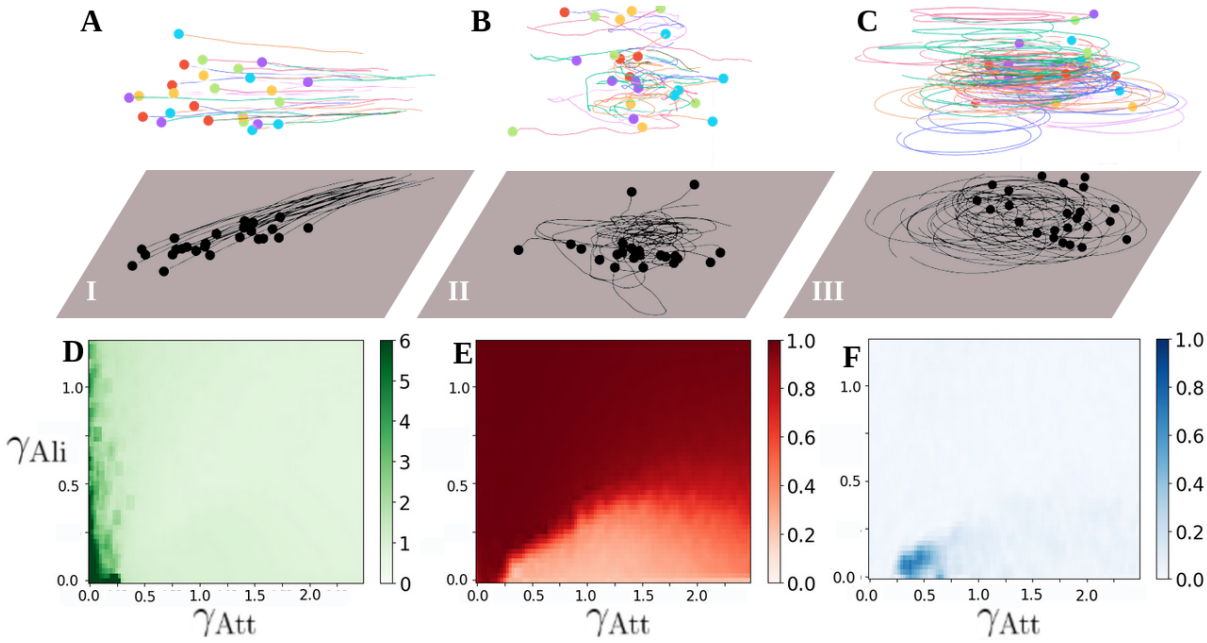

Fig. 1. 3D-trajectories and their projections on the XY-plane of the collective states displayed by a swarm of 25 UAVs flying in free space without any specified altitude when each UAV only interacts with its most influential neighbor: A) schooling, (B) swarming, and (C) milling. (D) Dispersion $D(t)$, (E) polarization $P(t)$, and (F) milling $M(t)$ for 50 UAVs, as a function of the intensity of the attraction γ_{Att} and alignment γ_{Ali}. The vertical interaction is present, but not modified between simulations. Each pixel value corresponds to a mean value of 100 simulations of 180 s with fixed interaction intensities.

circular arena). Removing the absolute value in (16) shows the clockwise or anticlockwise direction of rotation.

We ran 100 simulations of 50 UAVs flying during 180 s for each value of γ_{Ali} and γ_{Att} and calculated the value of these three observables D, P, and M. Fig. 1 shows the density plots for each observable in the corresponding $(\gamma_{\mathrm{Ali}}, \gamma_{\mathrm{Att}})$-plane.

For each observable, we introduce a threshold allowing us to build a phase plane characterizing the different collective behaviors [15]. When attraction and alignment are sufficiently strong to prevent dispersion ($D < 5.5$), three behavioral phases can be identified:

I. Schooling: $P > 0.75$, $M < 0.4$ (red region in Fig. 2). Drones maintain a tight formation and fly in the same direction. Schooling behavior is useful for navigation along a given trajectory, or for keeping a compact swarm.

II. Swarming: $P < 0.75$, $M < 0.4$ (green). Drones are not polarized but remain cohesive. Swarming behavior serves for tasks such as mapping and delivery, in which the swarm must cover a large area in a distributed manner.

III. Milling: $P < 0.75$, $M > 0.4$ (blue). Drones describe a rotating pattern around an arbitrary point, regardless of the sense of rotation. This pattern is only observed in large swarms where agents interact only with very close neighbors, and not with agents moving in the opposite direction. Milling behavior is especially useful in non-stoppable vehicles, such as fixed-wing UAVs, for altitude gain or loss, with a limited horizontal dispersion.

Fig. 2 shows that the schooling phase occupies the upper $2/3$ of the $(\gamma_{\mathrm{Ali}}, \gamma_{\mathrm{Att}})$-plane, indicating that schooling occurs provided a minimal alignment force is given. If alignment

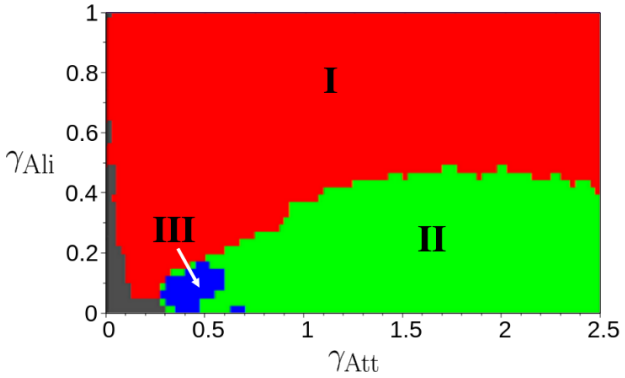

Fig. 2. Phase diagram corresponding to the collective motion patterns shown in Fig. 1: (I) Schooling phase (red), where $P > 0.75$ and $M < 0.4$, (II) Swarming phase (green), where $P < 0.75$ and $M < 0.4$, and (III) Milling phase (blue), where $P < 0.75$ and $M > 0.4$. In the gray region (bottom-left corner) dispersion is very high ($D > 5.5$) and no collective patterns are observed. The parameter values for these simulations were: $d_0^{\mathrm{Ali}} = 1\,\mathrm{m}$, $l_{\mathrm{Ali}} = 2.5\,\mathrm{m}$, $d_0^{\mathrm{Att}} = 1.25\,\mathrm{m}$, $l_{\mathrm{Att}} = 2.75\,\mathrm{m}$, $\gamma_{\mathrm{Acc}} = 0.25$, $d_0^{\mathrm{Acc}} = 1\,\mathrm{m}$, $l_{\mathrm{Acc}} = 2.5\,\mathrm{m}$, $\gamma_{\mathrm{z}} = 0.25$, $d_0^{\mathrm{z}} = 1.25\,\mathrm{m}$, $L_{\mathrm{z}_2} = 1.75\,\mathrm{m}$.

is not sufficiently strong (with γ_{Ali} larger than 0.25–0.5, depending on γ_{Att}), the swarm of drones adopts a swarming behavior unless the attraction is in a specific range of small values ($\gamma_{\mathrm{Att}} \approx 0.25$–$0.6$). There, the swarm adopts a milling formation. In fact, the milling behavior is a specific motion pattern that is very close to the swarming behavior, but more coordinated in rotation around the barycenter of the group. If both interaction forces are weak, the swarm loses its cohesion and disperses ($D > 5.5$).

The phase diagram can change with the size of the swarm, the number of influential neighbors taken into account,

or the parameters of the interaction functions [15]. Still, phase diagrams are a powerful tool for implementing phase transitions, either manually, or through a decision process.

B. Modulation of swarm cohesion along the vertical axis

The model presented in Section II allows the drones to fly at any altitude between 0 and 5 m (height of the upper limit of the arena). The vertical distance of separation d_0^z introduced in Eq. 3 leads the drones to stay at that vertical distance from each other. The model simulations shown in Section III-A were carried out with $d_0^z = 1.25$ m so that vertical interactions do not affect the 2D behavioral patterns. The model also makes it possible to produce other behaviors along the vertical axis. Fig. 3 shows that drones can be driven to split vertically or fly all at a given altitude.

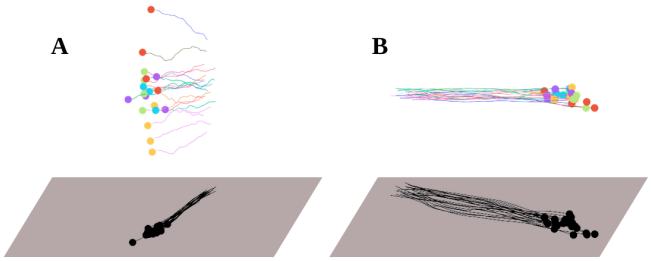

Fig. 3. 3D trajectories of a schooling swarm of 25 UAVs flying in an unbounded space, (A) vertically dispersed, and (B) with a specified altitude.

This flexibility in adopting different moving patterns can bring benefits in specific scenarios of drone swarm navigation, e.g., to release agents that are blocked in local minima (during a migration, or in front of non-convex obstacles), and therefore deserves a deeper exploration in a 3D volume.

Fig. 4 shows the distribution of the vertical position z of drones under different conditions, both during experimental tests and in simulations. When no target altitude is specified, both UAVs and agents self-organize at a vertical distance of about 1.25 m from each other: see the bumps at $z = 1.5$, 3, and 4.25 m, confined by the upper border at $z = 5$ m. On the other hand, when a target altitude is specified, here at $z = 3$ m, the two UAVs manage to stay at this altitude, while the three agents are forced to separate themselves horizontally because of the additional term $(\delta v_i^z)^{\text{nav}}$ in Eq. 3.

The choice to carry out experimental tests only with 2 drones with a specified altitude is due to the constraints imposed by the size of the flight arena (see Fig. 5), which confines drones horizontally, and therefore increases vertical repulsion when there are too many drones.

C. Using collective phases for an operational control of the swarm

In operational contexts, the main challenge consists in guiding the swarm. At any time, the operator must be able to change the navigation order, stop the swarm, or track its progress, while controlling its moving direction. The navigation terms in Eqs. (2)–(4) allow the operator to guide the swarm toward a specified area by exploiting the self-organizing properties of the flocking model. These terms

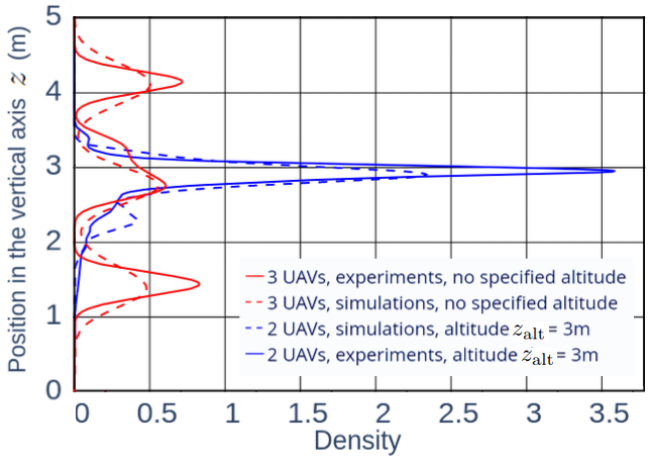

Fig. 4. Distribution of the vertical position of the UAVs inside a cylindrical arena of 5 m height in two conditions: without specifying a target altitude (3 UAVs, red lines), and with a target altitude $d_0^z = 3$ m (2 UAVs, blue lines). We performed 5 experiments of ∼8 min in the flight arena (solid lines) and 50 runs of 8 min in model simulations (dashed lines).

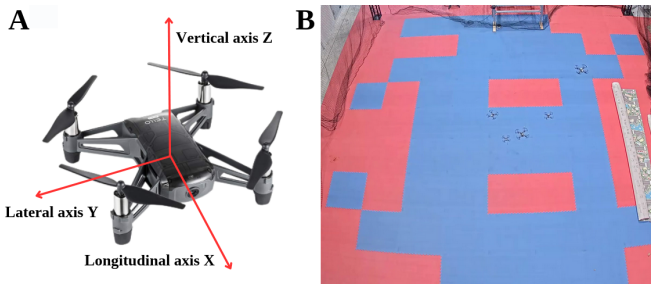

Fig. 5. (A) Experimental UAV (a Tello EDU®; www.ryzerobotics.com) used in our experiments. (B) Swarm of drones in the flight arena (a 3.25-meter radius circle is added in simulation for wall interaction and safety).

define a vector field whose direction and intensity are subject to dynamic changes in the environment (wind, obstacles) and to commands sent by the operator. Using vector fields allows for preserving the swarm formation while moving toward a desired location. Moreover, guidance by vector fields is readily applicable to border and obstacle avoidance [16], [17], [18].

In a common case of flying within a navigation corridor, the field is often uniform (locally and within the corridor), thus creating additional alignment in the calculation of the agents' heading, and therefore between nearby drones. To what extent does this field influence the polarization of the swarm remains to be measured, but a pattern close to the frontier of the schooling domain will show a higher level polarization if the swarm is subject to an additional locally uniform guiding field.

Beyond the context of flying within a navigation corridor, where the swarm will mostly perform schooling (with a high level of polarization), the attraction to a specific area, the calculation of a dynamic field for obstacle avoidance, or even a constant arbitrary term to favor exploration of an unknown area, can be helped by adopting a specific phase. Keeping in mind that the model can be extended in terms

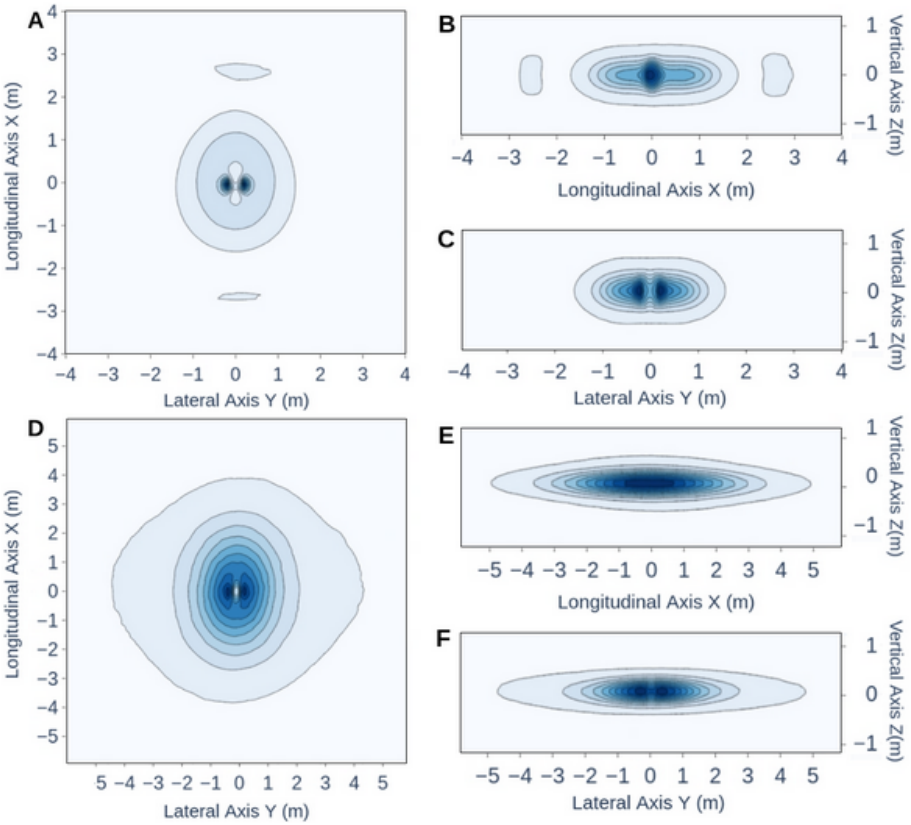

Fig. 6. Density map of the relative position of the most influential neighbor in the system of reference of the focal agent defined by the longitudinal, lateral, and vertical axes X, Y, and Z respectively (Fig. 5A). (A) XY-plane, (B) XZ-plane, and (C) YZ-plane. During 90% of the time, the most influential neighbor is found within 2 m around the focal agent in the XY-plane, and within 0.48 m above or below the focal agent in the YZ-plane. Density map of all the agents in (D) the XY-plane, (E) the XZ-plane, and (F) the YZ-plane. Note that the spatial scales used in (ABC) and (DEF) are different. In all figures, the density is normalized to 1, and contour lines are equispaced by 0.1. Results are based on 100 simulations of 300 s, with 50 agents flying in an unbounded arena, and no specified altitude. The parameter values for the simulations are: $\gamma_{\mathrm{Ali}} = 0.8$, $d_0^{\mathrm{Ali}} = 1\,\mathrm{m}$, $l_{\mathrm{Ali}} = 2.5\,\mathrm{m}$, $\gamma_{\mathrm{Att}} = 1.2$, $d_0^{\mathrm{Att}} = 1.25\,\mathrm{m}$, $l_{\mathrm{Att}} = 2.75\,\mathrm{m}$.

of distances, we can find examples of motion patterns for a variety of scenarios. The exploration of an unknown zone, with an unspecified border ([19], [20]), or a simple case of search and rescue can be favored by using a swarming pattern, scaled to the characteristic size of the environment, with an individual appeal to unexplored subareas, guaranteeing an optimal dispersion in the horizontal and vertical domains. While the algorithm has not been tested on fixed-wings drones, the Milling phase could be used by those drones for staying in a wind updraft or just decreasing their altitude, while keeping a specific position in the horizontal plane. Moreover, the algorithms can ensure in such cases coordination with a varying number of agents. Ultimately, a reactive algorithm confers significant benefits in dynamic or unknown environments [21]. By implementing perception at the local scale, agents can interact with the environment, and impact other agents by influencing their dynamics. The way information spreads across the swarm, from peer to peer, can be useful even without communication, the same way it allows biological flocks to perceive and collectively avoid a threat.

IV. Reducing the Searching Zone of Influential Neighbor

In the biological model, fish interact with at most 1 or 2 neighbors [12], [13]. The social interaction strategy consists in selecting the neighbors to interact with according to the influence they exert on the focal fish. The influence of a neighbor is defined as the absolute value of its contribution to the instantaneous heading change of the focal fish, $|\delta\phi(t)|$ [13]. Thus, the most influential neighbor is the one having the highest contribution. With the two additional interactions, the choice was made to measure the influence as the heading angle change weighted with the longitudinal and vertical speed change (Eq. 10). This formulation allows us to modulate the collective interactions between UAVs so that only one influential neighbor is required to produce an aligned and cohesive swarm.

By selecting the influential neighbors in terms of each interaction, the swarm tends to be more aligned and rigid, justifying the choice of only using one influential neighbor.

The following results show the importance of selecting the most influential neighbor. We focus our analysis on the schooling phase (see Part III for the description of the collective phases) in which the swarm is polarized, without

specifying the flight altitude to the agents, or a direction to follow.

Figs. 6ABC show the density distribution of the position of the most influential neighbor of a focal UAV flying inside the swarm in its 3D reference system in the schooling phase (see the reference axes shown in Fig. 5). The central finding is the highly compact nature of this distribution in relation to proximity to the focal agent. Vertically, the most influential agent is located within a distance of 1 meter from the focal agent, while horizontally, at a comparable range on either side of the agent. This distribution is a direct consequence of the choice of the interaction parameters, as they have a strong impact on the relative positions between drones. Characteristic distances between drones can be set to a given value by simply adjusting the ranges and the distances of equilibrium defining the interactions functions [13]. Other parameters, such as the intensity of interactions γ_{Ali}, γ_{Att}, γ_{Acc}, and γ_z, also have a deep impact on the shape of the density map.

The density distribution of the most influential neighbor only reaches local maxima in two symmetrical points. The separation between the UAVs along the vertical axis is also ensured, and UAVs are rarely found directly above each other. This is necessary because of the columns of the air disturbances that multirotors generate at close range, and is the result of adjusting the parameters between the vertical interaction and the rest of the social interactions.

A prominent point of this distribution, and especially the one in Fig. 6, is that it can help in designing an effective swarm of UAVs. The fact that the most influential neighbor can be found in a restricted and localized zone has a clear impact on the choice of an onboard visual or close-range communication system. Moreover, if we consider the distribution of all neighbors around a focal agent, one can see that they rarely obstruct the line of sight between this focal agent and its most influential neighbor. A schooling pattern is essential in any UAV deployment scenario, as it guarantees the best stability, in terms of alignment and variation of distance between agents, as well as the adaptability of the swarm to a vector field. The other phases, as well as the tweaking of parameters that control the vertical interaction, can be adapted to an operational need, from corridor tracking to surveillance or exploration.

V. Conclusion

In this article, we presented a 3D bio-inspired flocking algorithm for a drone swarm, based upon a previously validated 2D model. This extension to 3D was proved to be effective, and after scaling it to the other interactions and the extra need for vertical separation in quadrotors, the resulting distribution around a focal agent satisfies safety needs in terms of coordination and separation. We also showed how the vertical interaction in the model affects the variables of observation and the way agents select their influential neighbor(s). Knowing where to look for an influential neighbor, and therefore acquiring important data to achieve coordinated collective motion, is key in designing an efficient swarm of UAVs. Finally, the collective motion patterns that can be obtained through the modification of a small amount of the model parameters were presented and can serve as indirect guiding strategies in various operational contexts. Future work will explore the ability of this UAV swarm flocking algorithm to ensure safe transitions between collective phases in different operational contexts and its deployment in a real swarm of dozens of UAVs, as in [22].

Acknowledgements

This work was supported by a grant from the University of Toulouse and the Région Occitanie / Pyrénées-Méditerranée to M. V., G. T and G. H., G. T., R. E. and C. S. were supported by the Agence Nationale de la Recherche (ANR-20-CE45-0006-1).

References

[1] D.C. Tsouros, *et al.*, "A Review on UAV-Based Applications for Precision Agriculture," *Information*, vol. 10:349, 2019.

[2] A. Tahir, *et al.*, "Swarms of Unmanned Aerial Vehicles — A Survey," *Journal of Industrial Information Integration*, vol. 16: 100106, 2019.

[3] M. Ayamga, *et al.*, "Multifaceted applicability of drones: A review," *Technological Forecasting and Social Change*, vol. 167: 120677, 2021.

[4] X. Zhou, *et al.*, "Swarm of micro flying robots in the wild," *Science Robotics*, vol. 7: 5954, 2022.

[5] J. Alonso-Mora, *et al.*, "Distributed multi-robot formation control in dynamic environments," *Autonomous Robots*, vol. 43, pp. 1079–1100, 2019.

[6] M. Dorigo, *et al.*, "Swarm Robotics: Past, Present, and Future [Point of View]," *Proceedings of the IEEE*, vol. 109, no. 4, pp. 1152–1165, 2021.

[7] M. Verdoucq, *et al.*, "Bio-inspired control for collective motion in swarms of drones," in *2022 International Conference on Unmanned Aircraft Systems (ICUAS)*, 2022, pp. 1626–1631.

[8] D.S. Calovi, *et al.*, "Collective response to perturbations in a data-driven fish school model," *Journal of The Royal Society Interface*, vol. 12: 20141362, 2015.

[9] D. Calovi, *et al.*, "Disentangling and modeling interactions in fish with burst-and-coast swimming reveal distinct alignment and attraction behaviors," *PLOS Computational Biology*, vol. 14: e1005933, 2018.

[10] R. Escobedo, *et al.*, "A data-driven method for reconstructing and modelling social interactions in moving animal groups," *Philosophical Transactions of the Royal Society B: Biological Sciences*, vol. 375: 20190380, 2020.

[11] "ROS2 (Robotic Operating System 2.0). Available at: https://github.com/ros2." [Online]. Available: https://github.com/ros2

[12] L. Jiang, *et al.*, "Identifying influential neighbors in animal flocking," *PLOS Computational Biology*, vol. 13: e1005822, 2017.

[13] L. Lei, *et al.*, "Computational and robotic modeling reveal parsimonious combinations of interactions between individuals in schooling fish," *PLOS Computational Biology*, vol. 16:e1007194, 2020.

[14] M. Moussaid, *et al.*, "Collective Information Processing and Pattern Formation in Swarms, Flocks, and Crowds," *Topics in Cognitive Science*, vol. 1, no. 3, pp. 469–497, 2009.

[15] W. Wang, *et al.*, "The impact of individual perceptual and cognitive factors on collective states in a data-driven fish school model," *Plos Computational Biology*, vol. 18: e1009437, 2021.

[16] F. Belkhouche, "Reactive Path Planning in a Dynamic Environment," *IEEE Transactions on Robotics*, vol. 25, pp. 902–911, 2009.

[17] F. Belkhouche, *et al.*, "Modeling and controlling 3D formations and flocking behavior of unmanned air vehicles," in *2011 IEEE International Conference on Information Reuse & Integration*, 2011, pp. 449–454.

[18] Z. Bilgin, *et al.*, "Panel method based path planning for fixed wing micro aerial vehicles," *13^{th} International Micro Air Vehicle Conference*, pp. 25–31, 2022.

[19] T. Verdu, *et al.*, "Flight patterns for clouds exploration with a fleet of UAVs," in *2019 International Conference on Unmanned Aircraft Systems*, 2019, pp. 231–237.

[20] G. Hattenberger, *et al.*, "Field report: Deployment of a fleet of drones for cloud exploration," *International Journal of Micro Air Vehicles*, vol. 14, 2022.

[21] X. Li, *et al.*, "Biologically inspired flocking of swarms with dynamic topology in uniform environments," in *IEEE Conference on Decision and Control*, 2007, pp. 2522–2527.
[22] G. Vásárhelyi, *et al.*, "Optimized flocking of autonomous drones in confined environments," *Science Robotics*, vol. 3: eaat3536, 2018.